Mammalian WDR12 is a novel member of the Pes1–Bop1 complex and is required for ribosome biogenesis and cell proliferation

Michael Hölzel,[1,4] Michaela Rohrmoser,[1] Martin Schlee,[1] Thomas Grimm,[1] Thomas Harasim,[1] Anastassia Malamoussi,[1] Anita Gruber-Eber,[1] Elisabeth Kremmer,[2] Wolfgang Hiddemann,[3,4] Georg W. Bornkamm,[1] and Dirk Eick[1]

[1]Institute of Clinical Molecular Biology and Tumour Genetics, [2]Institute of Molecular Immunology, and [3]Clinical Cooperative Group Acute Leukemia, National Research Center for Environment and Health (GSF), 81377 Munich, Germany
[4]Department of Internal Medicine III, University Hospital Grosshadern, Ludwig-Maximilians-University, 81377 Munich, Germany

Target genes of the protooncogene c-*myc* are implicated in cell cycle and growth control, yet the linkage of both is still unexplored. Here, we show that the products of the nucleolar target genes Pes1 and Bop1 form a stable complex with a novel member, WDR12 (PeBoW complex). Endogenous WDR12, a WD40 repeat protein, is crucial for processing of the 32S precursor ribosomal RNA (rRNA) and cell proliferation. Further, a conditionally expressed dominant-negative mutant of WDR12 also blocks rRNA processing and induces a reversible cell cycle arrest. Mutant WDR12 triggers accumulation of p53 in a p19ARF-independent manner in proliferating cells but not in quiescent cells. Interestingly, a potential homologous complex of Pes1–Bop1–WDR12 in yeast (Nop7p–Erb1p–Ytm1p) is involved in the control of ribosome biogenesis and S phase entry. In conclusion, the integrity of the PeBoW complex is required for ribosome biogenesis and cell proliferation in mammalian cells.

Introduction

Coordination of cell growth and cell division is a fundamental prerequisite for proliferating cells to remain constant in size (Polymenis and Schmidt, 1999; Fingar et al., 2002; Schmidt, 2004). Ribosome biogenesis, the major constituent of cellular growth, accounts for up to 80% of the energy consumption of dividing cells (Thomas, 2000). Disturbances in the ribosome synthesis pathway must be detected and coupled with cell cycle progression to prevent premature cell divisions. The fact that the oncogenic transcription factor c-Myc efficiently promotes proliferation might result from its capacity to positively regulate both ribosome biogenesis and cell cycle progression (Schmidt, 1999, 2004). Yet it remains unclear how c-Myc achieves this concerted action.

The *c-myc* protooncogene is implicated in proliferation, cell growth, differentiation, and apoptosis (Oster et al., 2002; Nilsson and Cleveland, 2003; Pelengaris and Khan, 2003; Schmidt, 2004). Deregulated expression is associated with a variety of human neoplasias. Several high throughput techniques have substantially extended the list of potential c-Myc target genes (Fernandez et al., 2003; Li et al., 2003; Patel et al., 2004). Transcriptional control by c-Myc has been reported on hundreds of genes (Coller et al., 2000; Guo et al., 2000; Schuhmacher et al., 2001). One major subset of target genes is involved in ribosome biogenesis and cell metabolism. Other gene products exert cell cycle control. Indeed, c-Myc is of pivotal importance to promote entry into and to prevent exit from the cell cycle (Eilers et al., 1991; Hölzel et al., 2001; Trumpp et al., 2001). On the other hand, constitutive expression of c-Myc mediates accumulation of cell mass (Schuhmacher et al., 1999; Kim et al., 2000). These findings suggest that c-Myc target genes physiologically act in concert to promote proliferation while ensuring the equilibrium between cell growth and cell cycle progression. However, the mechanisms that survey balanced cell divisions in mammalian cells remain largely unexplored. Nevertheless, several recent studies have considerably enlarged our knowledge. Intriguing links between nucleolar function and cell cycle control have emerged.

Conditional deletion of the ribosomal protein gene S6 in mice impeded cell cycle entry of liver cells after partial hepatectomy (Volarevic et al., 2000). Surprisingly, hepatocytes of starved mice regained their baseline cell size after feeding despite the lack of ribosomal protein S6. Thus, ribosome biogenesis is essential for proliferation but not for accumulation of cell

Correspondence to Dirk Eick: eick@gsf.de

Abbreviations used in this paper: rRNA, ribosomal RNA; siRNA, small interfering RNA.

The online version of this article includes supplemental material.

The Journal of Cell Biology, Vol. 170, No. 3, August 1, 2005 367–378
http://www.jcb.org/cgi/doi/10.1083/jcb.200501141

mass. Several mechanisms have been proposed that couple nucleolar function to cell cycle control. Interestingly, they all imply the tumor suppressor p53.

First, the Mdm2 oncoprotein mediates the proteasomal degradation of p53 (Stommel et al., 1999; Tao and Levine, 1999a; Boyd et al., 2000). The p19ARF tumor suppressor disrupts Mdm2–p53 binding, sequesters the former to the nucleolus, and thus stabilizes p53 (Tao and Levine, 1999b; Weber et al., 1999). Another mechanism proposes nuclear export of p53 via the nucleolus for subsequent degradation in the cytoplasm (Sherr and Weber, 2000). In fact, Mdm2–p53 complexes are found in conjunction with the ribosomal proteins L5 and L11 (Marechal et al., 1994; Lohrum et al., 2003; Zhang et al., 2003). These findings suggest that Mdm2–p53 complexes assemble with ribosomes for their CRM1-dependent nuclear export. Indeed, it was shown that a subset of ribosomes contained cytoplasmic p53 covalently linked to 5.8S ribosomal RNA (rRNA; Fontoura et al., 1992, 1997). Hence, the nucleolar export model directly couples nucleoplasmic p53 levels to the functional state of ribosome biogenesis. This model received substantial support as it was demonstrated that DNA damage by localized UV irradiation of cell nuclei failed to trigger stabilization of the tumor suppressor p53 unless the nucleolus was affected (Rubbi and Milner, 2003). Moreover, the literature confirms that all p53-inducing stresses cause nucleolar disruption besides the ones that act downstream of the nucleolus such as the proteasome and nuclear export inhibitors MG132 and leptomycin B, respectively (Rubbi and Milner, 2003). Recently, it was shown that the ribosomal proteins L5, L11, and L23 negatively regulate Mdm2 activity (Lohrum et al., 2003; Zhang et al., 2003; Dai and Lu, 2004; Jin et al., 2004). Proliferating cells incorporate L5, L11, and L23 into functional ribosomes. Disturbances in the ribosome synthesis pathway, in contrast, result in the accumulation of free ribosomal proteins. The subsequent inhibition of Mdm2 by L5, L11, and L23 causes activation of p53.

Hence, the nucleolus is a common stress sensor of pivotal importance in the p53 response. Therefore, precise knowledge about ribosome biogenesis is required to unravel the signals that transmit nucleolar disturbance to the cell cycle. Several genetic and proteomic studies in yeast provided intriguing details of the complex molecular machinery needed for ribosome synthesis (Fatica and Tollervey, 2002; Fromont-Racine et al., 2003; Saveanu et al., 2003; Takahashi et al., 2003). As an example, yeast Nop7p (Yph1p) has been implicated in the control of ribosome biogenesis and DNA replication via its interaction with origin recognition complex proteins (Du and Stillman, 2002). Two other proteins, Erb1p and Ytm1p, have been copurified with Nop7p in a small core complex. Remarkably, Bop1, the human homologue of Erb1p, plays a role in rRNA processing and cell cycle control (Strezoska et al., 2002). Dominant-negative mutants of Bop1 interfered with proper rRNA processing and provoked a p53-dependent cell cycle arrest (Pestov et al., 2001). More recently, Bop1 was shown to interact with Pes1, the mammalian homologue of Nop7p (Lapik et al., 2004). This indicates that a set of evolutionarily conserved proteins might coordinate ribosome biogenesis with DNA replication in mammalian cells.

Previously, we identified a considerably large number of c-Myc target genes involved in rRNA processing (Schlosser et al., 2003). It received our particular attention that c-Myc up-regulated the expression of *pes1*, *bop1*, and *wdr12*. Mammalian WD repeat protein 12 (WDR12) is the putative homologue of yeast Ytm1p. It is tempting to speculate that in analogy to yeast, Pes1, Bop1, and WDR12 might function in an evolutionarily conserved complex. Thus, c-Myc dependent up-regulation of these three factors might promote the formation of a subcomplex that is important for the assembly of larger preribosomal complexes and the cross talk between ribosome biogenesis and proliferation control.

However, the biological functions of mammalian WDR12 are yet unknown. WDR12 mRNA is ubiquitously expressed during embryogenesis and high levels are found in the thymus and testis of adult mice. In addition, GST pull-down experiments revealed an interaction with Notch1-IC, therefore sug-

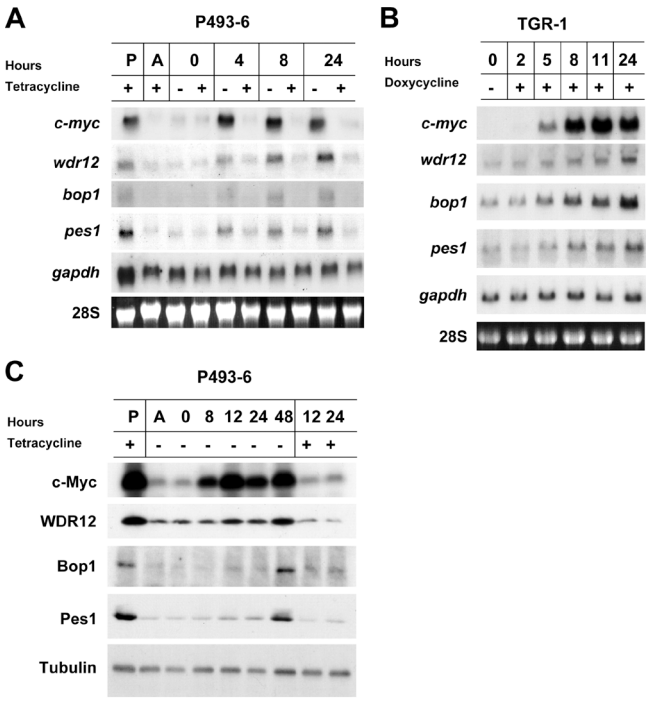

Figure 1. **c-Myc controls endogenous *wdr12* expression.** (A) Northern blot analysis of *wdr12* expression in the human B cell line P493-6 carrying a tetracycline-controllable *c-myc* gene. Removal of tetracycline from the culture medium by several washes with PBS strongly stimulated exogenous *c-myc* expression. As a control, separate cultures were treated equally, however, in the presence of tetracycline. Equal amounts of total RNA were hybridized with radioactively labeled probes specific for human *c-myc*, *wdr12*, *bop1*, and *pes1*. Expression of *gapdh* was not affected by c-Myc. Bottom panel shows ethidium bromide staining as loading control. P, proliferating cells; A, arrested cells. (B) Northern blot analysis of WDR12 expression in TGR-1 rat fibroblasts. TGR-1 cells were stably transfected with a construct encoding a doxycycline-inducible human *c-myc* gene. Cells were arrested by contact inhibition to reduce endogenous *c-myc* levels. Addition of doxycycline to the culture medium strongly activated exogenous *c-myc* expression. Equal amounts of total RNA were hybridized with radioactively labeled probes specific for human *c-myc* and rodent *wdr12*, *bop1*, and *pes1*. Expression of *gapdh* was not affected by c-Myc. Bottom panel shows ethidium bromide staining as loading control. (C) Western blot analysis of WDR12 expression in P493-6 cells. Cells were treated as described in A. Immunodetection was performed with antibodies against c-Myc (N-262), WDR12 (1B8), Bop1, Pes1, and α-tubulin (DM1A).

gesting a role in early stages of primary T cell differentiation (Nal et al., 2002). The high homology between mammalian WDR12 and yeast Ytm1p prompted us to study the role of WDR12 in ribosome biogenesis and cell proliferation.

Results

c-Myc up-regulates WDR12

First, we analyzed the expression of WDR12 in a human B cell line (P493-6) harboring a *c-myc* tet-off system (Schuhmacher et al., 1999). Proliferation of P493-6 cells is *c-myc* dependent. After the induction of *c-myc*, *wdr12* mRNA was similarly up-regulated as *bop1* and *pes1* (Fig. 1 A). To rule out cell line–specific observations, we established TGR-1 rat fibroblasts carrying a *c-myc* tet-on system. Addition of doxycycline to the culture medium induced rapid and strong *c-myc* expression resulting likewise in up-regulation of endogenous *wdr12*, *bop1*, and *pes1* mRNA levels (Fig. 1 B). Further, we raised monoclonal antibodies specific against human WDR12, Bop1, and Pes1. Proliferating P493-6 cells expressed high levels of all three proteins in contrast to arrested cells (Fig. 1 C). Consistently, endogenous WDR12, Bop1, and Pes1 accumulated subsequent to conditional c-Myc expression.

WDR12 is a nuclear protein with predominant nucleolar localization

To determine the cellular localization of endogenous WDR12, we performed indirect immunofluorescence. WDR12 localized to the nucleolus and nucleoplasm in various cell lines such as U2OS (Fig. 2 A, top), HeLa, and WI-38 (not depicted). Further, human diploid fibroblasts were cotransfected with expression constructs coding for WDR12-eYFP and eCFP-nucleophosmin fusion proteins. WDR12-eYFP exhibited diffuse nucleoplasmic distribution, strong accumulation within the nucleolus, and nucleolar colocalization with nucleophosmin (Fig. 2 A, bottom). Similar results were obtained in rodent fibroblasts (unpublished data). Interestingly, nucleolar localization was also reported for GFP- and HA-tagged forms of yeast Ytm1p, the potential homologue of mammalian WDR12 (Ouspenski et al., 1999; Huh et al., 2003). Hence, our data provide for the first time experimental evidence that mammalian WDR12 and yeast Ytm1p are potential homologues exhibiting similar subcellular distribution.

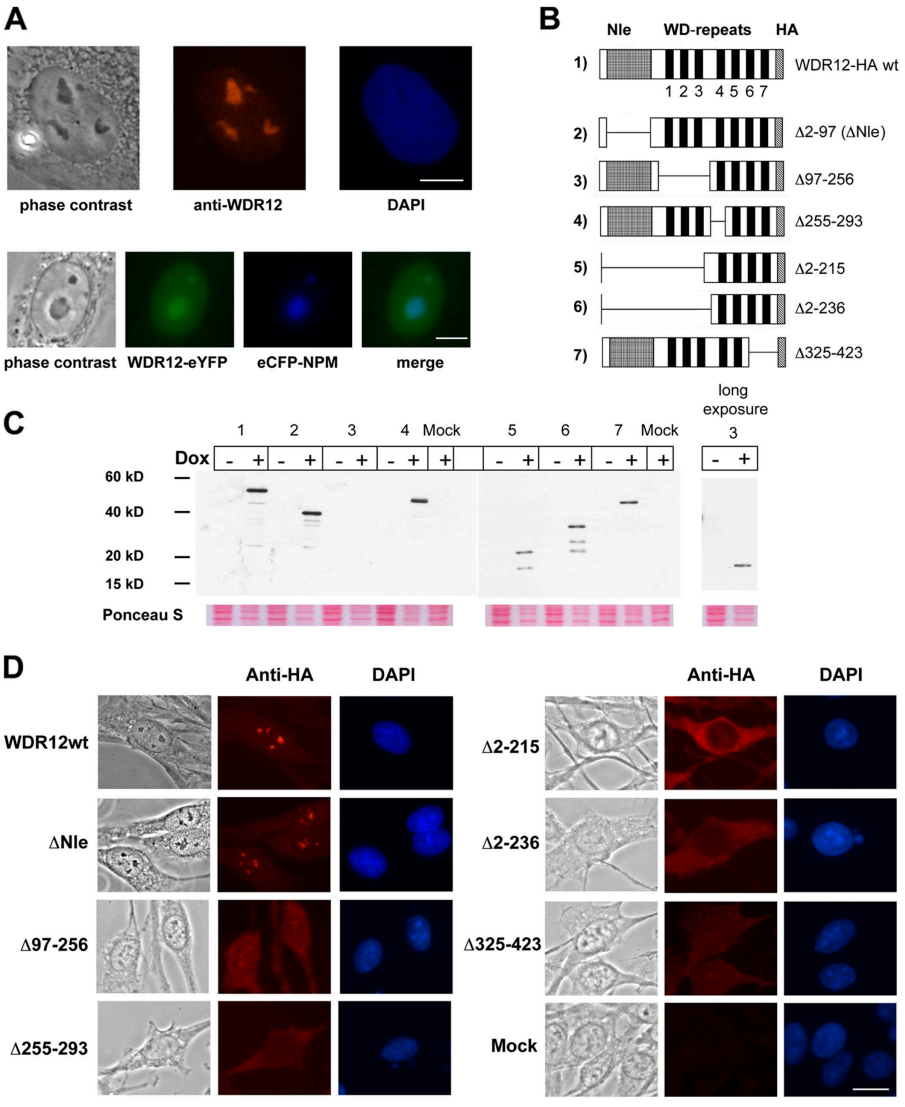

Figure 2. **Subcellular localization and mutagenesis of WDR12.** (A) Endogenous WDR12 was visualized by indirect immunofluorescence in PFA-fixed U2OS cells (top). Nuclei were counterstained with DAPI. Human diploid fibroblasts were transiently cotransfected with constructs encoding the WDR12-eYFP and eCFP-Nucleophosmin fusion proteins. A representative image of a transfected cell is shown (bottom). (B) Outline of domain-specific mutagenesis of WDR12. Several truncation mutants of HA-tagged human WDR12 were generated and cloned into pRTS plasmids allowing doxycycline-dependent gene expression. (C) Western blot analysis of wild-type and mutant WDR12-HA in stably transfected TGR-1 fibroblasts. The indicated polyclonal cell lines were treated with doxycycline for 24 h (+) or left untreated (−). Bottom panel shows Ponceau S staining as loading control. (D) Analysis of subcellular localization of WDR12 mutants. TGR-1 cells were stably transfected with the indicated constructs and treated with doxycycline for 24 h. Methanol-fixed cells were analyzed by indirect immunofluorescence. Representative images are shown in each panel. Nuclei are visualized by DAPI staining. As control, cells expressing luciferase were equally analyzed (Mock). Bars: (A) 10 μm; (D) 20 μm.

Mutational analysis of WDR12

Next, we aimed to assess the biological functions of WDR12 by mutational analysis. WDR12 belongs to the family of WD repeat proteins that are generally thought to regulate protein–protein interactions (Smith et al., 1999). These factors consist of several copies of a defined amino acid motif, the WD domain. WDR12 contains seven COOH-terminal WD repeats, as predicted by BMERC analysis (Nal et al., 2002). Crystallographic studies of other factors with seven WD repeats revealed that the WD domains form a "propeller-like" structure composed of seven "blades" (Wall et al., 1995). The NH_2 terminus of WDR12 has significant similarity to the NH_2-terminal part of Notchless, a protein implicated in the modulation of Notch signaling in *Drosophila melanogaster* (Royet et al., 1998; Nal et al., 2002). This defined structural organization of WDR12 prompted us to generate a panel of different truncation mutants (Fig. 2 B). We established stable polyclonal cell lines of TGR-1 rat fibroblasts that express WDR12 wild-type or mutant forms together with eGFP from a bidirectional promoter in a doxycycline-dependent manner (unpublished data). After doxycycline treatment, >95% of the cells were eGFP positive, as monitored by flow cytometry in each experiment. Levels of HA-tagged WDR12 mutants were determined by immunoblotting (Fig. 2 C). Some mutant forms of WDR12-HA were detected at the calculated molecular size, whereas others exhibited multiple products at a significantly lower size (Fig. 2 C, lanes 3, 5, and 6). This is most likely due to rapid degradation of unstable mutant forms. Interestingly, all unstable WDR12 mutants lack the first three WD domains.

Further, we examined the cellular localization of WDR12 mutants by immunofluorescence (Fig. 2 D). As expected, the HA-tagged wild-type form of WDR12 localized to the nucleolus. Surprisingly, only WDR12 lacking the NH_2-terminal Notchless-like domain (WDR12ΔNle) also exhibited predominant nucleolar staining. The remaining WDR12 mutants dispersed in the cytoplasm and nucleoplasm.

WDR12ΔNle inhibits proliferation

To test whether wild-type WDR12 or mutants affect proliferation, we seeded equal numbers of stable TGR-1 cell cultures at low density in the presence of doxycycline. After 6 d, the number of cells was determined in multiples and compared with the mean cell count of a mock cell line expressing luciferase (Fig. 3 A). Enforced expression of exogenous wild-type WDR12 neither impaired nor promoted cell proliferation. However, deletion of the NH_2-terminal Notchless-like domain resulted in a strongly reduced cell count. We excluded an increase of apoptosis by Annexin V staining using flow cytometry as a potential explanation for this observation (unpublished data). Hence, the block of proliferation in response to enforced WDR12ΔNle expression is due to cell cycle arrest rather than increased cell death. To support this hypothesis, we performed BrdU light assays (Pestov and Lau, 1994). Thereby we investigated whether enforced WDR12ΔNle expression elicits a reversible cell cycle arrest. In brief, dividing cells that incorporate BrdU into their DNA become highly photosensitive if they are additionally labeled with Hoechst dye and irradiated with light. Hence, cell cycle–arrested cells are protected from increased photosensitivity and survive BrdU light treatment. Conditional WDR12ΔNle expression efficiently rescued TGR-1 cells from BrdU light treatment, whereas wild-type WDR12 failed to do so (Fig. 2 B). As controls, we generated stable cell lines expressing wild-type Bop1, Bop1Δ and Bop1N2, two previously described dominant-negative mutants of Bop1 (Pestov et al., 2001; Strezoska et al., 2002).

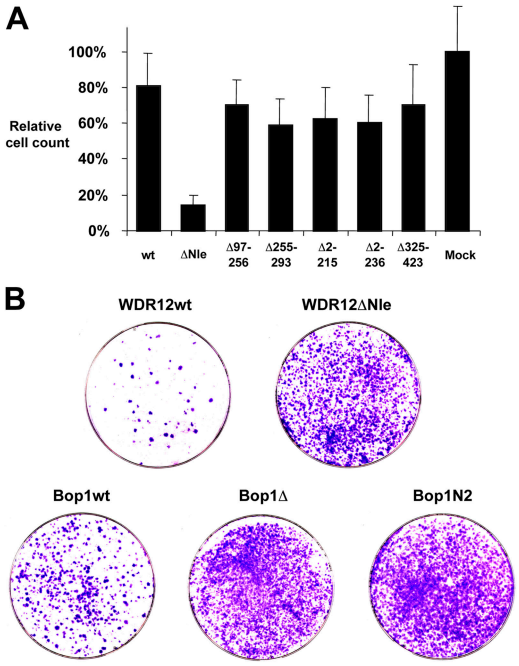

Figure 3. **WDR12ΔNle inhibits cell proliferation and elicits a reversible cell cycle arrest.** (A) Equal numbers of TGR-1 cells stably transfected with the indicated constructs were seeded in multiples in the presence of doxycycline. After 6 d, cells were trypsinized and counted by trypan blue exclusion. Final cell counts of the indicated cell lines were compared with a mock cell line that expresses luciferase. Histograms depict the relative cell counts after 6 d. Error bars indicate SD. (B) Reversible cell cycle arrest by WDR12ΔNle overexpression. Stably transfected TGR-1 cells were seeded at low density and treated with doxycycline for 30 h to induce expression of the specified constructs. Subsequently, cells were incubated with 100 μM BrdU for 48 h to label proliferating cells. Visible light irradiation in the presence of 2 μM Hoechst 33258 selectively kills cells that have incorporated BrdU into their DNA. Arrested cells survive BrdU light treatment and give rise to cell colonies after withdrawal of doxycycline. Images show representative BrdU light assays conducted with the indicated cell lines.

To further examine the impact of WDR12ΔNle expression on cell proliferation, we performed cell cycle analysis using flow cytometry (Fig. S1, available at http://www.jcb.org/cgi/content/full/jcb.200501141/DC1). Overexpression of Bop1Δ, as previously shown, led to accumulation of cells in G1 and reduction in S phase (Pestov et al., 2001). Albeit the strong inhibitory effect of WDR12ΔNle on cell proliferation, we observed only slight alterations of the cell cycle distribution and a less pronounced accumulation in G1 than in Bop1Δ-expressing cells. Hence, our data suggests that in addition to a complete G1 arrest, cells may also exhibit delayed overall cell cycle progression in response to WDR12ΔNle and probably also Bop1Δ.

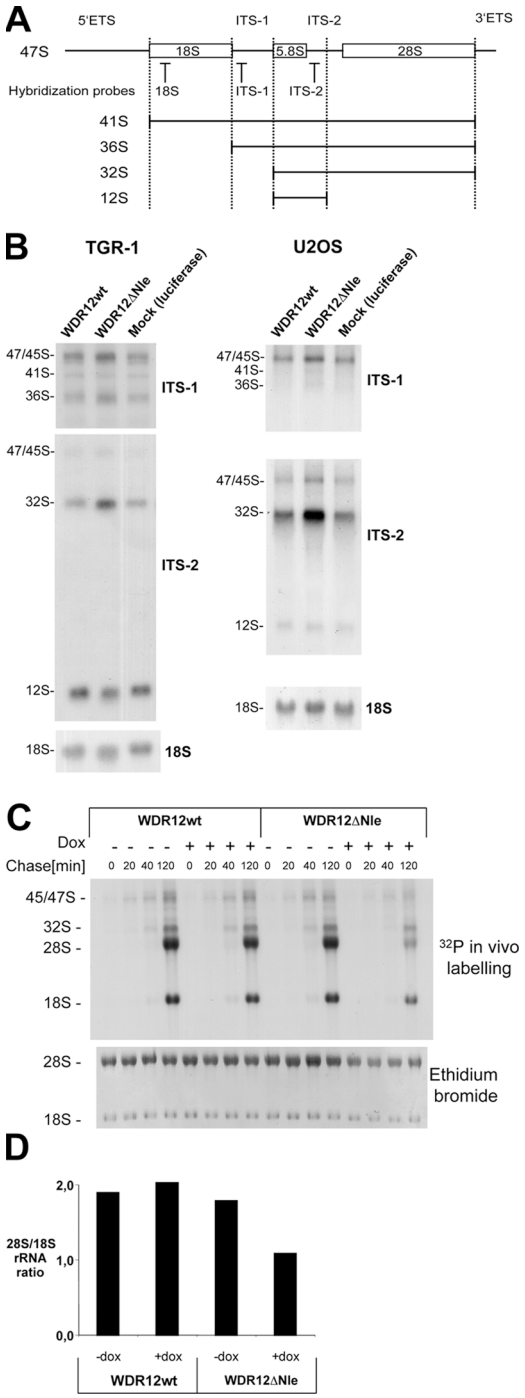

Figure 4. **WDR12ΔNle expression affects rRNA processing.** (A) Diagram of the primary 47S rRNA transcript and the major rRNA intermediates. Positions of the hybridization probes are depicted. ETS, external transcribed spacer; ITS, internal transcribed spacer. (B) Northern blot analysis of rRNA precursors in WDR12ΔNle-expressing TGR-1 and U2OS cells. Indicated cell lines were treated with doxycycline for 30 h. Equal amounts of total RNA were hybridized with probes specific for the ITS1 and ITS2 of rRNA intermediates. As loading control, blots were incubated with a probe specific for 18S rRNA. (C) WDR12ΔNle expression impairs formation of mature 28S rRNA. Asynchronously growing TGR-1 cells were treated with or without doxycycline for 24 h. Cells were pulse labeled with ^{32}P-orthophosphate for 45 min and chased in regular medium as indicated. (D) Ratio of 28S/18S rRNA at 120 min after metabolic labeling with ^{32}P-orthophosphate as described in C.

Mutants lacking the first three WD40 repeats in addition to the deleted Notchless-like domain failed to block proliferation. Thus, disrupted integrity of the WD repeat domains rescued the inhibitory effect of WDR12ΔNle. Noteworthily, these mutants also exhibited aberrant subcellular distribution. Our data suggest that the dominant-negative phenotype of WDR12ΔNle depends on its nucleolar localization.

WDR12ΔNle interferes with rRNA processing

From the aforementioned results we reasoned that WDR12ΔNle might confer its inhibitory effect on cell proliferation via interference with rRNA processing. Besides, there is accumulating evidence in the literature supporting our notion. Yeast Ytm1p, the potential homologue of WDR12, interacts with Erb1p and Nop7p (Yph1p) in a complex that links ribosome biogenesis with DNA replication (Du and Stillman, 2002). Bop1 and Pes1, the candidate mammalian homologues of Erb1p and Nop7p, both play a role in rRNA processing and, moreover, also physically interact (Strezoska et al., 2002; Lapik et al., 2004). Therefore, we investigated the levels of different rRNA species in WDR12ΔNle-expressing TGR-1 and U2OS cells by Northern blot analysis (Fig. 4, A and B). Total RNA was probed with sequences specific for the ITS1 and ITS2 (internal transcribed spacer) of rRNA intermediates (Fig. 4 A). WDR12ΔNle-expressing cells accumulated the 32S rRNA precursor (Fig. 4 B). In another set of experiments, we studied the impact of WDR12ΔNle on rRNA processing in TGR-1 cells by metabolic ^{32}P in vivo labeling (Fig. 4 C). The production of mature 28S rRNA was severely reduced resulting from an inefficient processing of the 32S rRNA precursor, as concluded from the decreased ratio of 28S/18S rRNA (Fig. 4 D). Synthesis of mature 18S rRNA was almost unaffected, as determined by the signal intensity of the 18S rRNA normalized to the total RNA loading. These results are in line with our Northern blot analysis. In conclusion, WDR12ΔNle primarily compromises ribosome biogenesis by blocking processing of the 32S rRNA precursor into mature 28S rRNA.

Endogenous WDR12 is required for rRNA processing and cell proliferation

To confirm the role of WDR12 in ribosome biogenesis and cell proliferation, we performed small interfering RNA (siRNA) knockdown experiments of endogenous WDR12. U2OS cell were transfected at day 0, 1, and 2 with either control or WDR12-specific siRNA. Expression of endogenous WDR12 was dramatically reduced, as monitored by Western blot analysis 2 d after the last transfection (Fig. 5 A). Moreover, proliferation of WDR12-depleted cells was severely impaired (Fig. 5 B). Further, we investigated the impact of WDR12 knockdown on ribosome biogenesis. Levels of precursor and mature rRNA species were determined by Northern blot analysis 2 d after the last siRNA transfection. WDR12-depleted cells exhibited accumulation of the 32S precursor rRNA and a concomitant reduction of the mature 28S rRNA (Fig. 5 C). To study more immediate effects of WDR12 knockdown on rRNA process-

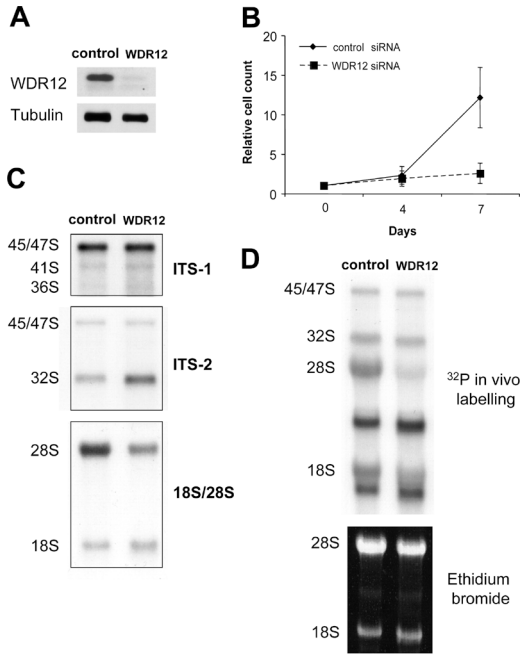

Figure 5. **Endogenous WDR12 is required for rRNA processing and cell proliferation.** (A) U2OS cells were transfected at day 0, 1, and 2 with either control or WDR12-specific siRNA. Endogenous WDR12 levels were analyzed by Western blot analysis 2 d after the last transfection. α-Tubulin is shown as a loading control. (B) U2OS cells were seeded in multiples at low density and treated as described in A. Cells were counted at days 0, 4, and 7. Error bars indicate SD. (C) U2OS cells were treated as in A and total RNA was harvested 2 d after the last transfection. Different rRNA species were visualized by Northern blot analysis using probes specific for human ITS-1, ITS-2, 28S, and 18S rRNA. (D) U2OS cells were transfected only twice at day 0 and 1 and metabolically labeled with ^{32}P-orthophosphate for 60 min at day 3. Subsequently, cells were incubated for 3 h in regular culture medium.

ing, cells were transfected only twice at day 0 and 1 and in vivo labeling of rRNA was performed 2 d later. Again, the production of the mature 28S rRNA was drastically compromised (Fig. 5 D). Notably, synthesis of the large 45/47S precursor was not affected, indicating that WDR12 is not involved in rRNA transcription. In conclusion, expression of dominant-negative WDR12ΔNle and depletion of endogenous WDR12 block rRNA processing of the 32S rRNA precursor and restrain cell proliferation.

WDR12ΔNle triggers accumulation of p53

Disruption of the nucleolus is a common feature of a variety of stresses such as DNA damage. It has been previously postulated that impairment of nucleolar function is the "common denominator" to mediate stabilization of p53 (Rubbi and Milner, 2003). Based on these findings, we explored the p53 response after enforced WDR12ΔNle expression in asynchronously proliferating TGR-1 cells (Fig. 6 A, top). Indeed, WDR12ΔNle in contrast to wild-type WDR12 mediated an accumulation of endogenous p53. The dominant-negative mutants Bop1Δ and Bop1N2 also stabilized p53. Thus, accumulation of p53 apparently is a common feature of compromised rRNA processing. Next, we investigated the conditions under which WDR12ΔNle mediates stabilization of p53. Total cell lysates of proliferating and arrested cells were analyzed by immunoblotting. Interestingly, p53 failed to accumulate in serum-starved cells (Fig. 6 A). Similarly, contact inhibition resulted in an alleviated p53 response. Equal expression of exogenous proteins was verified by immunoblotting (unpublished data). Likewise, we studied the endogenous p53 response by immunofluorescence and examined the percentage of p53-positive cells (Fig. 6 B). In proliferating TGR-1 fibroblasts, WDR12ΔNle provoked an accumulation of p53 in almost 60% of the cells (Fig. 6 C). Intensity and percentage of p53-positive nuclei diminished in the case of contact inhibition and serum starvation. Consistent results were obtained for Bop1Δ and Bop1N2. In summary, p53 accumulation in response to inhibition of rRNA processing is especially pronounced in proliferating cells compared with quiescent cells. We also tested whether the accumulation of p53 was associated with phosphorylation at serine 15. Interestingly, we observed an increase of serine 15–phosphorylated p53 congruently with the overall accumulation of p53 (Fig. S2, available at http://www.jcb.org/cgi/content/full/jcb.200501141/DC1). Further, we investigated the WDR12ΔNle-mediated p53 response by analyzing the transcriptional activation of the p53-responsive gene p21 using quantitative real-time PCR (Fig. 6 D). Induction of p21 mRNA resembled the accumulation of p53 in response to WDR12ΔNle expression (Fig. 6 A, top; and Fig. 6 D).

As previously demonstrated, Bop1Δ and Bop1N2 elicited a p53-dependent cell cycle arrest that was attenuated by the coexpression of the human papillomavirus protein E6, a ubiquitin ligase targeting p53 for degradation (Scheffner et al., 1993). In line with these studies, WDR12ΔNle-induced cell cycle arrest was alleviated in TGR-1 cells stably transfected with HA-tagged E6 (Fig. 6 E). Interestingly, overexpression of wild-type Bop1 was accompanied with increased p53 levels. This corresponds to the weak but significant rescue of wild-type Bop1 in the BrdU light assay (Fig. 3 B).

Accumulation of p53 is independent of the tumor suppressor p19ARF

To explore the mechanism of p53 accumulation mediated by interference with rRNA processing, we studied the role of p19ARF in this response. The tumor suppressor p19ARF sequesters Mdm2 to the nucleolus and triggers stabilization of p53 (Sherr and Weber, 2000). In unstressed cells, nucleoplasmic Mdm2 targets p53 for degradation via ubiquitination. Overexpression of p19ARF inhibits rRNA processing in a p53-independent manner and binds to 5.8S rRNA. Therefore, p19ARF might be required for the accumulation of p53 in response to WDR12ΔNle. Stable polyclonal cell lines of p19ARF−/− and p53−/− MEFs were generated that conditionally express wild-type WDR12, WDR12ΔNle, and Bop1Δ. Upon exogenous gene activation, endogenous p53 levels were visualized by immunoblotting (Fig. 6 F). Indeed, overexpression of WDR12ΔNle and Bop1Δ provoked accumulation of p53 in p19ARF−/− cells. Hence, the tumor suppressor p19ARF is dispensable for an appropriate p53 response elicited by inhibition of rRNA processing.

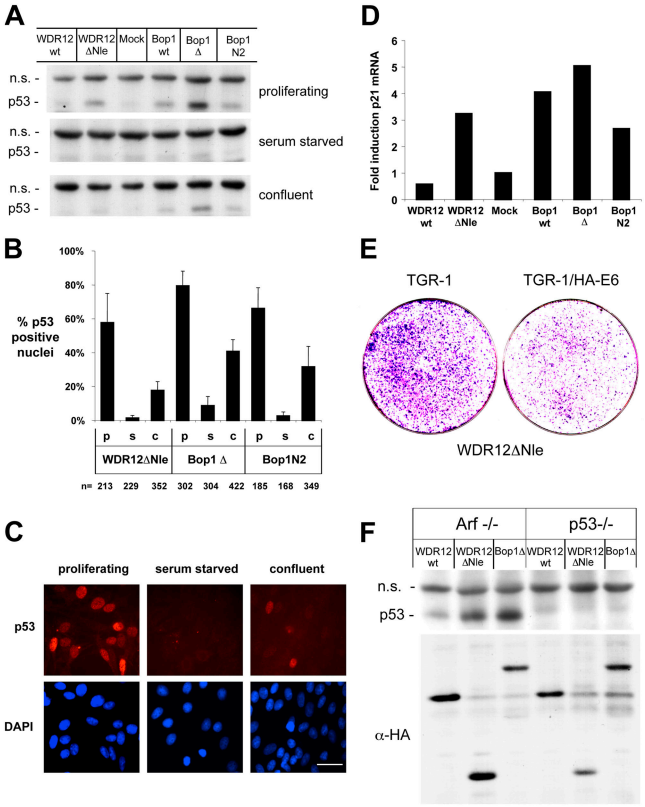

Figure 6. **WDR12ΔNle provokes accumulation of the tumor suppressor p53.** (A) Western blot analysis of endogenous p53 levels. TGR-1 cells were stably transfected with the indicated constructs. Asynchronously proliferating, serum starved (72 h), and contact inhibited cells were treated with doxycycline for 24 h to induce expression of the respective products. Equal amounts of whole cell lysates were analyzed by immunoblotting using anti-p53 (Pab122) antibodies. The top band corresponds to a nonspecific signal, as verified in p53−/− cells (F). The nonspecific band indicates equal loading in addition to Ponceau S staining (not depicted). Identical expression of the HA-tagged constructs was visualized by immunoblotting with anti-HA (3F10) antibody (not depicted). (B) Percentage of p53-positive nuclei in TGR-1 cells upon induction of the dominant-negative mutants WDR12ΔNle, Bop1Δ, and Bop1N2. Asynchronously proliferating (p), serum-starved (s), and confluent (c) cells were analyzed by immunofluorescence as described in C. Numbers of examined cells are indicated at the bottom. Error bars indicate SD of the percentage of p53-positive nuclei cells per high power field. (C) Analysis of the endogenous p53 response to WDR12ΔNle expression by indirect immunofluorescence. Asynchronously proliferating, serum-starved (72 h), and contact-inhibited cells were treated with doxycycline for 24 h to induce WDR12ΔNle. Cells were fixed in methanol and stained with anti-p53 (Pab122). Cell nuclei were counterstained with DAPI. Representative images are shown. Bar, 60 μm. (D) Asynchronously proliferating TGR-1 cells stably transfected with the indicated constructs were treated with doxycycline for 24 h. Levels of p21 mRNA were analyzed by quantitative real-time PCR. Fold induction was normalized to the expression of aldolase. (E) WDR12ΔNle-mediated reversible cell cycle arrest is alleviated by functional impairment of the endogenous p53 response in TGR-1 cells stably transfected with the HA-tagged human papillomavirus protein E6. Identical numbers of TGR-1 and TGR1-HA-E6 cells both conditionally expressing WDR12DNle were subjected to BrdU light treatment as described. Images show representative methanol-fixed and GIEMSA-stained cell cultures. (F) Accumulation of p53 is independent of p19ARF. p19ARF−/− and p53−/− MEFs were stably transfected with the indicated constructs. Asynchronously proliferating cells were treated with doxycycline for 24 h and equal amounts of whole cell lysates were analyzed by immunoblotting with anti-p53 antibody.

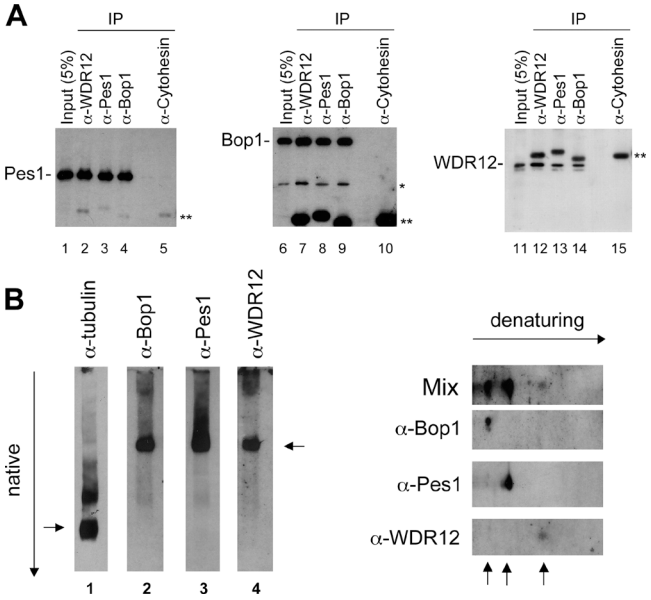

Figure 7. **Endogenous WDR12 forms a stable complex with endogenous Pes1 and Bop1.** (A) Asynchronously proliferating U2OS cells were harvested and immunoprecipitations were performed using antibodies against WDR12, Pes1, Bop1, and Cytohesin, as an IgG1 isotype control. Subsequently, immunoblotting was performed using antibodies against Pes1, Bop1, and WDR12, respectively. *, non specific band; **, IgG heavy chain. (B) Total cell lysates of U2OS cells were separated by native gel electrophoresis. Endogenous Bop1, Pes1, WDR12, and α-tubulin were visualized by immunoblotting. Arrows indicate complexes containing the respective factor. In another set of experiments, native gel electrophoresis was followed by a second denaturing gel electrophoresis. Afterwards, Bop1, Pes1, and WDR12 were detected by immunoblotting using the respective antibodies as mix or alone. Anti-Pes1 usually generates a very strong signal compared with the weaker signal of the anti-WDR12 antibody. (right) Arrows indicate Bop1, Pes1, and WDR12, respectively.

WDR12 forms a stable complex with Bop1 and Pes1

Because the potential yeast homologues Nop7p (Yph1p), Erb1p, and Ytm1p form a stable core complex (Harnpicharnchai et al., 2001; Du and Stillman, 2002), we finally asked whether endogenous Pes1, Bop1, and WDR12 also constitute a stable complex in mammalian cells. Monoclonal antibodies were raised against all three proteins and applied in immunoprecipitation experiments. Each protein was specifically immunoprecipitated and also coimmunoprecipitated the two other proteins (Fig. 7 A). Even though our results strongly suggested that the proteins participate in common complexes, the number and abundance of endogenous complexes containing Pes1, Bop1, and WDR12 remained unknown. Therefore, we performed native gel electrophoresis using stringent cell lysis conditions to unravel stable core complexes. Strikingly, immunoblot analysis of all three proteins exhibited a single major band at the same height of the native gel, indicating the existence of one stable complex. Overexpression of the respective exogenous components of the complex resulted in faster migrating bands indicating free nonincorporated proteins (unpublished data). Moreover, the presence of each protein in this complex was verified by subsequent second dimension gel electrophoresis under denaturing conditions followed by immunoblotting.

Hence, endogenous Pes1, Bop1, and WDR12, like their potential yeast homologues, form a stable core complex in mammalian cells (PeBoW complex).

Discussion

Using cDNA microarrays, we previously identified numerous c-Myc target genes involved in ribosome biogenesis and demonstrated a global role for c-Myc in the control of efficient rRNA processing (Schlosser et al., 2003). Pes1, Bop1, and WDR12 are the products of three target genes that received our particular attention. Pes1 and Bop1 are directly interacting proteins involved in rRNA processing and proliferation (Strezoska et al., 2002; Lapik et al., 2004). In addition, the respective yeast homologues Nop7p (Yph1p) and Erb1p have been copurified in preribosomal complexes (Harnpicharnchai et al., 2001; Du and Stillman, 2002; Saveanu et al., 2003). Moreover, Nop7p and Erb1p assemble in a small subcomplex together with Ytm1p (Harnpicharnchai et al., 2001; Du and Stillman, 2002). Intriguingly, WDR12 is the most likely homologue of Ytm1p in mammalian cells. Proteomic and genetic studies suggest a role for Ytm1p in the maturation of the 60S ribosomal subunit and chromosomal stability (Ouspenski et al., 1999; Harnpicharnchai et al., 2001). Mammalian WDR12 has been cited as a Notch1-IC interacting protein; however, its biological functions remain unexplored (Nal et al., 2002).

In this study, we demonstrate that WDR12 is a crucial factor in the mammalian ribosome biogenesis pathway that forms a stable complex with Pes1 and Bop1. We were able to show that deletion of the evolutionarily conserved Notchless-like domain of WDR12 results in a dominant-negative phenotype. Interfering with WDR12 function inhibits rRNA processing at specific stages and blocks cell proliferation. Furthermore, we provide evidence that accumulation of the tumor suppressor p53 is a common phenomenon of impaired rRNA processing in a proliferation-dependent manner.

WDR12 and ribosome biogenesis

A genome-wide GFP-tagging approach in yeast revealed nuclear and nucleolar localization of Ytm1p (Huh et al., 2003). We demonstrated that endogenous WDR12, WDR12-HA, and WDR12-eYFP fusion proteins were uniformly distributed in the nucleoplasm and accumulated within the nucleolus. The similar localization of Ytm1p and WDR12 supports the notion that both proteins are indeed homologous proteins. Our subcellular localization experiments using a monoclonal antibody that detects endogenous WDR12 protein appear more reliable than overexpression studies that have reported a more homogeneous nuclear distribution of eGFP-WDR12 in HeLa cells (Nal et al., 2002).

To determine whether WDR12 is a nucleolar factor required for ribosome biogenesis, we developed a series of truncation mutants based on sequence-predicted domains. We aimed to identify dominant-negative phenotypes by screening for proliferation defects. Our results show that the NH_2-terminal Notchless-like domain is not required for nucleolar localization of WDR12. In contrast, disrupting the integrity of the seven WD repeats and therefore the potential propeller-like structure caused aberrant nucleoplasmic and cytoplasmic distribution. Among mutants that were tested, only WDR12ΔNle suppressed cell proliferation and inhibited proper rRNA processing. Prominent accumulation of the 32S prerRNA indicates defective processing in ITS2. Therefore, the NH_2-terminal Notchless-like domain probably mediates pivotal interactions in preribosomal complexes, as its removal severely impairs prerRNA processing. Importantly, our siRNA knockdown experiments confirmed that endogenous WDR12 is required for processing of the 32S precursor rRNA without affecting the synthesis of the 45S/47S primary transcript. Collectively, these results demonstrate that mammalian WDR12 functions in the maturation of the 60S ribosomal subunit.

Inhibition of prerRNA processing and cell cycle control

Overexpression of WDR12ΔNle strongly restrained cell proliferation without significant increase in apoptosis. Conducting BrdU light assays, we demonstrated that WDR12ΔNle imposes a reversible cell cycle arrest on TGR-1 rat fibroblasts. Similar results have been reported on dominant-negative mutants of Bop1 and Pes1, respectively (Pestov et al., 2001; Lapik et al., 2004). Likewise, depletion of endogenous WDR12 severely inhibited cell proliferation. Thus, inhibition of prerRNA processing is coupled with repression of cell proliferation. Noteworthily, changes in cell cycle distributions were less pronounced as expected from the proliferation and BrdU light assays. Hence, our data suggest that in addition to a complete cell cycle arrest, the overall cell cycle progression may also be delayed. The precise nature of this interesting observation needs further investigation.

In a hallmark study, Pestov et al. (2001) demonstrated a link between the tumor suppressor p53 and the response to "nucleolar stress." Impairment of endogenous p53 by the human papillomavirus protein E6 abrogated the Bop1Δ-mediated cell cycle arrest. Congruently, WDR12ΔNle-triggered cell cycle arrest was alleviated by the coexpression of HA-E6. Further, dominant-negative mutants of WDR12 and Bop1 provoked considerable accumulation of nuclear p53 and transcriptional activation of the target gene p21. Our results are in line with the study of Rubbi and Milner (2003), supporting the model that compromised functionality of the nucleolus is the basic principle of p53 stabilization in response to diverse stresses. Several intriguing molecular mechanisms have been unravelled that might contribute concertedly or independently to the overall increase in nuclear p53. First, Mdm2–p53 complexes assembled with ribosomes argue for a nucleolar transit of p53 for subsequent cytoplasmic degradation. On the other hand, the ribosomal proteins L5, L11, and L23 exert negative regulation on Mdm2 if they are not incorporated into functional preribosomal complexes (Lohrum et al., 2003; Zhang et al., 2003; Dai and Lu, 2004; Jin et al., 2004). Inhibition of prerRNA processing might result in an oversupply of free L5, L11, and L23 and may thus facilitate stabilization of p53 by blocking Mdm2 function. Our observations are consistent with either model, because insufficient rRNA processing reduces the production and export of mature ribosomes in the same way as the demand for the ribosomal proteins L5, L11, and L23. From the aforementioned results, we reasoned

that the impact of WDR12ΔNle or Bop1Δ expression on p53 accumulation should be dependent on the rate of ribosome biosynthesis. Quiescent TGR-1 cells virtually shut down ribosome biogenesis (unpublished data). Hence, WDR12ΔNle and Bop1Δ are not expected to additionally increase nuclear p53 levels in arrested cells. Indeed, we were able to demonstrate that dominant-negative mutants of WDR12 and Bop1 failed to elicit p53 accumulation in serum-starved cells. TGR-1 fibroblasts grown to confluency gradually cease from the active cell division cycle. Again, the p53 response provoked by WDR12ΔNle, Bop1Δ, and Bop1N2 expression was significantly diminished in confluent compared with subconfluent cell cultures. Hence, inhibition of rRNA processing by dominant-negative mutants is a p53-inducing stress that depends on active ribosome biosynthesis. Interestingly, we also found a congruent increase of p53 phosphorylated at serine 15. Further investigation is needed to determine whether it reflects concomitant baseline phosphorylation of accumulated p53 or a specific signaling cascade mediated by disturbed rRNA processing. A recent study showed that human WI-38 fibroblasts accumulated p53 under growth-restricting conditions such as serum starvation and confluency (Bhat et al., 2004). Evidently, TGR-1 rat fibroblasts differ in this aspect from WI-38 cells. The precise explanation remains unclear. TGR-1 cells, however, are immortalized rodent cells that must have acquired genetic aberrations to overcome senescence and therefore might behave differently when challenged by unfavorable growth conditions. Despite this obvious discrepancy, we conclude that WDR12ΔNle, Bop1Δ, and Bop1N2 have no or little effect on the baseline p53 levels under growth-restricting conditions. Conclusively, proliferating cells require functional integrity of the nucleolus to prevent accumulation of p53.

The tumor suppressor p19ARF regulates stability of p53 via sequestration of Mdm2 to the nucleolus (Sherr and Weber, 2000). In addition, overexpression of p19ARF impairs rRNA processing (Sugimoto et al., 2003). Thus, p19ARF is a reasonable candidate to meditate the p53 response triggered by WDR12ΔNle and Bop1Δ. Our results, however, demonstrate that p19ARF is not required for accumulation of p53 provoked by dominant-negative mutants of ribosome synthesis factors.

Finally, we demonstrated that endogenous Pes1, Bop1, and WDR12 interact with each other in coimmunoprecipitation assays. Moreover, native gel electrophoresis revealed that all three proteins constitute only one major complex (PeBoW complex). In yeast, several studies showed that the potential homologous proteins Nop7p (Yph1p), Erb1p, and Ytm1p form a stable trimeric core complex (Harnpicharnchai et al., 2001; Du and Stillman, 2002). Potentially, the mammalian PeBoW complex may also exist as a trimeric core complex; however, we still cannot rule out that other factors may participate in the PeBoW complex. Most likely, the PeBoW complex is a stable subcomponent of larger preribosomal particles. Thus, previous studies in yeast and our data suggest that this core complex is evolutionarily conserved and its integrity is crucial for ribosome biogenesis and cell proliferation. It will be of outstanding interest to unravel whether the mammalian PeBoW complex directly plays a role in processes other than ribosome biogenesis, such as cell cycle control.

Similarly to DNA replication, cells are obliged to duplicate the translational machinery within each cell division cycle. Thus, intact ribosome biogenesis is crucial for normal and malignant cell proliferation. For decades, nucleolar morphology has served pathologists as a reliable indicator of malignancy. Aberrations in the protein synthesis machinery have been frequently implicated in cancer development (Ruggero and Pandolfi, 2003; Holland et al., 2004). Now, intriguing connections between cell cycle control, tumor suppressors, and nucleolar function have emerged. Exploration of individual factors is required to unravel the complex molecular machinery of ribosome synthesis and its role in tumor pathogenesis. Noteworthily, a recent study demonstrated that Pes1 enhances colony formation of SV40 large T-antigen immortalized cells (Maiorana et al., 2004). Mammalian ribosome synthesis factors might be directly implemented in malignant transformation apart from their function in ribosome synthesis. Therefore, it will be exciting to unravel positive and negative regulators of ribosome synthesis and their respective impact on tumor pathogenesis. Comparison of ribosome biogenesis and cell growth control in noncancerous and cancerous cells will be a promising approach to identify novel therapeutic targets. Specific inhibition of ribosome biogenesis might provide a nongenotoxic chemotherapy in addition to the classic chemotherapeutic drugs.

Materials and methods

Plasmids

Human *wdr12* cDNA was cloned into the EcoRV site of pUC18-HA tag using the following primers: 5′-GCCACCATGGCTCAGCTCCAAACACG-3′ and 5′-TGCCCCAACATGGGAAGTGGTAG-3′. A consensus Kozak sequence was added in front of the start codon. pUC18-HA tag was generated by cloning the following linker into the XbaI and HindIII sites of pUC18: 5′-TCTAGAGGCCTCACTGGCCGGCGATATCGGTTACCCTTATGATGTGCCAGATTATGCCTAAGGCCAGTGAGGCCAAGCTT-3′. pUC18-HA tag provides a COOH-terminal HA tag. *Wdr12*-HA was cloned via SfiI sites into pRTS-1, a single episomal plasmid enabling tight doxycycline-dependent gene expression. The bidirectional promoter of pRTS-1 plasmids controls the expression of eGFP and *wdr*12-HA wild type or mutants in a doxycycline-dependent manner. Human *c-myc* cDNA was flanked with SfiI sites and cloned into pRTS-1. Mouse HA-*bop1*, HA-*bop1Δ*, and *bop1N2* cDNAs were provided by D. Pestov (University of Illinois, Chicago, IL) and cloned into pRTS-1 plasmids. Human *wdr12* cDNA was cloned into pGEX-2T coding for a GST-WDR12 fusion protein. HA-E6 cDNA was provided by M. Scheffner (University of Konstanz, Constance, Germany) and cloned into pRTS-1 and pLXSP plasmids. *Wdr12*-eYFP and eCFP-nucleophosmin expression constructs were created by cloning *wdr12* and *nucleophosmin* into pEYFP-N1 and pECFP-C1 plasmids (CLONTECH Laboratories, Inc.), respectively. *Nucleophosmin* cDNA was provided by A. Lamond (University of Dundee, Dundee, UK).

Production of mAbs

Approximately 50 μg of GST-WDR12 fusion protein was injected both i.p. and subcutaneously into Lou/C rats using CPG2006 (TIB MOLBIOL) as adjuvant. After an 8-wk interval, a final boost was given i.p and subcutaneously 3 d before fusion. Fusion of the myeloma cell line P3X63-Ag8.653 with the rat immune spleen cells was performed according to standard procedures. Hybridoma supernatants were tested in a solid phase immunoassay. A monoclonal mouse mAb specific for the GST part of the fusion protein (M-GST 2C8, IgG1; Forschungzentrum für Umwelt und Gesundheit Research Centre [GSF]) was coated over night at a concentration of 3 μg/ml. After blocking with nonfat milk, the GST-WDR12 fusion protein or an irrelevant GST fusion protein was incubated, followed by the hybridoma supernatants. Bound rat mAbs were detected with a cocktail of biotinylated mouse mAbs against the rat IgG heavy chains, thus avoiding IgM mAbs. The biotinylated mAbs were visualized with peroxidase-labeled Avidin (Alexis) and *o*-phenylenediamine as chromogen in the peroxidase reaction.

A rat mAb against GST, binding to another epitope of the GST fusion protein (GST-6G9; GSF), served as a positive control.

The hybridoma designated WDR12-1B8 was stably subcloned and used for further analysis. The immunoglobulin isotype was determined using mAbs against the rat IgG heavy chains and light chains. The WDR12 (1B8) mAb has the IgG subclass IgG1. mAbs against human Pes1 (8E9) and Bop1 (6H11) were generated by using the following peptides coupled to ovalbumin (H.R. Rackwitz, Peptide Specialty Laboratories GmbH, Heidelberg, Germany): Pes1, AGSEKEEEARLAALEEQRMEGK; Bop1, SRGAGRTAAPSVRPEK. The Pes1 (8E9) and Bop1 (6H11) mAbs have the IgG subclass IgG1. Besides slight modifications, hybridoma cell lines were generated and supernatants were tested as described in this section. Generation of the anti-cytohesin antibody was described previously (Geiger et al., 2000).

Cell culture, transfections, and stable selection

TGR-1 rat fibroblasts, U2OS osteosarcoma cells, and p53−/− and p19ARF−/− MEFs were cultured in DME with 8% FBS (BioSer) at 8% CO_2. TGR-1 fibroblasts were provided by J. Sedivy (Brown University, Providence, RI), p53−/− MEFs were provided by G. Fingerle-Rowson (University Hospital Cologne, Cologne, Germany), and p19ARF−/− MEFs were provided by C.J. Sherr (Howard Hughes Medical Institute, St. Jude Children's Research Hospital, Memphis, TN). P493-6 cells were cultured in RPMI with 10% FBS at 5% CO_2. TGR-1 and U2OS cells, $\sim 7 \times 10^5$, were transfected with 4 μg pRTS-1 plasmids using polyfect (QIAGEN). Stable polyclonal cell cultures were selected in the presence of 200 μg/ml hygromycin B (TGR-1 and U2OS) or 1 μg/ml puromycin (TGR-1) for 10 to 14 d. Induction of conditional gene expression was performed with 1 μg/ml doxycycline. The percentage of eGFP-positive cells was monitored by FACS analysis. Human diploid fibroblasts were transfected by electroporation with 10 μg of plasmid DNA.

siRNA transfection

The day before transfection, $\sim 5 \times 10^4$ to 10^5 U2OS cells were seeded in 6-well plates. 5 μl of 20 μM control or WDR12-specific siRNA were diluted in 150 μl Optimem (Invitrogen). 150 μl Optimem containing 5 μl Oligofectamine (Invitrogen) was added and incubated for 15 min. Finally, 600 μl Optimem was added and applied to cells after aspiration of the culture medium. Cells were incubated for 5–6 h. The following sequences (sense) were used: WDR12, CGUACGUUUCCGUGGGCAAdTdT; Control (nonspecific siRNA), UUCUCCGAACGUGUCACGUdTdT.

Immunoblotting and immunofluorescence

TGR-1 and P493-6 cells were directly lysed in SDS-loading buffer (50 mM Tris-HCl, 100 mM DTT, 2% SDS, 0.1% bromophenol blue, and 10% glycerol). Total cell lysates were separated on SDS-PAGE gels and blotted on nitrocellulose membranes (GE Healthcare). Equal loading was verified by Ponceau S staining. Immunodetection was performed with anti-c-Myc (N-262; Santa Cruz Biotechnology, Inc.), anti-WDR12 (1B8), anti-Pes1, anti-Bop1, anti–α-tubulin (DM1A; Dianova), anti-HA (3F10; Roche), anti-p53 (Pab240; BD Biosciences), and anti–phospho-p53-Ser15 (Cell Signaling Technology Inc.).

For immunofluorescence, cells were grown on coverslips and fixed in ice-cold methanol for 10 min and air dried. Alternatively, cells were fixed in 4% PFA for 10 min and permeabilized with PBS/Tween 0.1% for 15 min at RT. Unspecific binding was blocked with PBS/10% FBS. p53 and HA-tagged WDR12 were detected with a 1:100 dilution of anti-p53 (Pab122; Dianova) and a 1:10 dilution of 3F10 hybridoma supernatant, respectively. Primary antibodies were incubated over night at 4°C in a humidified chamber. Cy3 or FITC-labeled secondary antibodies (Dianova) were incubated for 30 min at RT. Nuclei were counterstained with DAPI (Sigma-Aldrich). Digital images were acquired using the Openlab acquisition software (Improvision) and a microscope (model Axiovert 200M; Carl Zeiss MicroImaging, Inc.) with 63× (1.15) and 100× (1.30) plan oil objectives connected to a 5 charge-coupled device camera (model ORCA-479; Hamamatsu).

BrdU light assay

BrdU lights assays were performed essentially as previously described (Pestov and Lau, 1994). In brief, stable polyclonal TGR-1 cells were seeded in the presence of 1 μg/ml doxycycline at a density of 10^5 cells per 100-mm well. 30 h after seeding, cells were incubated with 100 μM BrdU and doxycycline for 48 h. Culture medium was then removed and replaced by medium containing doxycycline and Hoechst 33258 at 2 μg/ml for 3 h. Finally, cells were placed on glass 11 cm above a 30-W fluorescent daylight bulb and irradiated from beneath for 15 min. Cells were washed in PBS two times and regular culture medium without doxycycline was added.

RNA analysis and ^{32}P in vivo labeling

Total RNA of P493-6 and TGR-1 cells was isolated using Trifast (PeqLab). 10 μg of total RNA was separated on a 1% agarose-formaldehyde gel and blotted on hybond N^+ membranes (GE Healthcare). The following ^{32}P end-labeled DNA oligonucleotides were used to visualize rRNA precursors: ITS-1 (rat specific), 5′-GGACCAGACCCGACACCCTGCCACCGCACACCTGTCCCGAAACCCCCT-3′; ITS-2 (rat specific), 5′-GCCCCGGGGAGCGGGCCCTGCGAGCAGACTCCCAGCCGCGCGACGCGA-3′; ITS-1 (human specific), 5′-CCTCCGCGCCGGAACGCGCTAGGTACCTGGACGGCGGGGGGGCGGACG-3′; ITS-2 (human specific), 5′-GCGGCGGCAAGAGGAGGGCGGACGCCGCCGGGTCTGCGCTTAGGGGGA-3′; 18S rRNA (human and rat specific), 5′-CACCCGTGGTCACCATGGTAGGCACGGCGACTACCATCGAAAGTTGATAG-3′; 28S (human and rat specific), 5′-CCAGCTATCCTGAGGGAAACTTCGGAGGGAACCAGCTACTAGATGGTTCG-3′.

For metabolic labeling of rRNA, TGR-1 and U2OS cells were preincubated in phosphate-free DME (GIBCO BRL) with dialyzed FBS (Sigma-Aldrich) for 30 min. The medium was then replaced by phosphate-free DME/10% dialyzed FBS containing 15 μCi/ml ^{32}P-orthophosphate (GE Healthcare). After 45 min, the radioactive medium was removed and cells were incubated in regular DME/10% FBS for 2 h. 10 μg of total RNA were separated on 1% agarose-formaldehyde gels. After electrophoresis, gels were placed on whatman-paper and dried at 80°C under vacuum suction. Dried agarose gels were exposed to regular x-ray films (Kodak) and rRNA was visualized by autoradiography. A PhosphoImager (Fuji) was used for the quantification of signal intensities.

Immunoprecipitation

3×10^7 cells were lysed in 1 ml lysis buffer (50 mM Tris-HCl, pH 8.0, 1% NP-40, 150 mM NaCl, phosphatase inhibitors, and protease inhibitors) at 4°C for 20 min. 20 μg of glass beads were washed twice with PBS and incubated with 100 μl of anti-WDR12, anti-Bop1, anti-Pes1, and anti-Cytohesin supernatant for 1 h at 4°C. Afterwards, beads were washed once in lysis buffer. Subsequently, beads were incubated with 100 μl of total cell lysate at 4°C for 5 h. Immunoprecipitations were then washed three times with lysis buffer at 4°C and were incubated at 95°C for 10 min in a 1:1 dilution of 2× SDS loading buffer and lysis buffer. Finally, 5 μl of the immunoprecipitations were separated by SDS-PAGE.

Quantitative real-time PCR

Asynchronously proliferating TGR-1 cells were treated with doxycycline for 30 h and total RNA was isolated using Trifast (PeqLab). cDNA was produced using 1 μg of total RNA using oligo(dT)-primers and M-MLV reverse transcriptase (Promega). Subsequently, cDNA was diluted at 1:100 for quantitative real-time PCR using a LightCycler PCR analysis system (Roche) according to the manufacturer's recommendations. The following primers were used for detection of rat p21 mRNA: 5′-TGTTCCACACAGGAGCAAAG-3′ and 5′-CTCTTGCAGAAGACCAATCG-3′. Quantitative real-time PCR of aldolase was performed for normalization using the following primers: 5′-GGTCACAGCACTTCGTCGCACAG-3′ and 5′-TCCTTGACAAGCGAGGCTGTTGGC-3′.

Native gel and two-dimensional gel electrophoresis

3×10^6 cells were lysed in 100 μl lysis buffer at 4°C for 20 min. 7.5 μl of 2× sample buffer (125 mM Tris-HCl, pH 6.8, 30% glycerol, and 0.02% bromphenol blue) was added to 7.5 μl of total cell lysate and separated by PAGE (6.5%) in the absence of SDS at 4°C. The voltage did not exceed 100 V during electrophoresis. Blotting was performed in the absence of methanol. Immunoblotting was performed as described in the Immunoblotting and immunofluorescence section. For two-dimensional gel electrophoresis, subsequently to native gel electrophoresis, the appropriate lanes were cut out from the gel and incubated in SDS-running buffer for 10 min. Afterwards, the strips were applied horizontally to second dimension SDS-PAGE (10%). Immunoblotting was performed as described in the Immunoblotting and immunofluorescence section.

Online supplemental material

Fig. S1 shows cell cycle analysis of WDR12 mutant–expressing cells. Fig. S2 shows analysis of p53 phosphorylation at serine 15 in response to dominant-negative WDR12. Online supplemental material is available at http://www.jcb.org/cgi/content/full/jcb.200501141/DC1.

We thank C.J. Sherr for p19ARF$^{-/-}$ fibroblasts, G. Fingerle-Rowson for p53$^{-/-}$ fibroblasts, J. Sedivy for TGR-1 rat fibroblasts, D.G. Pestov for *bop1* cDNA, A.I. Lamond for *nucleophosmin* cDNA, and M. Scheffner for HA-E6 cDNA.

This work was supported by the Deutsche Forschungsgemeinschaft (EI 216/8-1).

Submitted: 27 January 2005
Accepted: 21 June 2005

References

Bhat, K.P., K. Itahana, A. Jin, and Y. Zhang. 2004. Essential role of ribosomal protein L11 in mediating growth inhibition-induced p53 activation. *EMBO J.* 23:2402–2412.

Boyd, S.D., K.Y. Tsai, and T. Jacks. 2000. An intact HDM2 RING-finger domain is required for nuclear exclusion of p53. *Nat. Cell Biol.* 2:563–568.

Coller, H.A., C. Grandori, P. Tamayo, T. Colbert, E.S. Lander, R.N. Eisenman, and T.R. Golub. 2000. Expression analysis with oligonucleotide microarrays reveals that MYC regulates genes involved in growth, cell cycle, signaling, and adhesion. *Proc. Natl. Acad. Sci. USA.* 97:3260–3265.

Dai, M.S., and H. Lu. 2004. Inhibition of MDM2-mediated p53 ubiquitination and degradation by ribosomal protein L5. *J. Biol. Chem.* 279:44475–44482.

Du, Y.C., and B. Stillman. 2002. Yph1p, an ORC-interacting protein: potential links between cell proliferation control, DNA replication, and ribosome biogenesis. *Cell.* 109:835–848.

Eilers, M., S. Schirm, and J.M. Bishop. 1991. The MYC protein activates transcription of the alpha-prothymosin gene. *EMBO J.* 10:133–141.

Fatica, A., and D. Tollervey. 2002. Making ribosomes. *Curr. Opin. Cell Biol.* 14:313–318.

Fernandez, P.C., S.R. Frank, L. Wang, M. Schroeder, S. Liu, J. Greene, A. Cocito, and B. Amati. 2003. Genomic targets of the human c-Myc protein. *Genes Dev.* 17:1115–1129.

Fingar, D.C., S. Salama, C. Tsou, E. Harlow, and J. Blenis. 2002. Mammalian cell size is controlled by mTOR and its downstream targets S6K1 and 4EBP1/eIF4E. *Genes Dev.* 16:1472–1487.

Fontoura, B.M., E.A. Sorokina, E. David, and R.B. Carroll. 1992. p53 is covalently linked to 5.8S rRNA. *Mol. Cell. Biol.* 12:5145–5151.

Fontoura, B.M., C.A. Atienza, E.A. Sorokina, T. Morimoto, and R.B. Carroll. 1997. Cytoplasmic p53 polypeptide is associated with ribosomes. *Mol. Cell. Biol.* 17:3146–3154.

Fromont-Racine, M., B. Senger, C. Saveanu, and F. Fasiolo. 2003. Ribosome assembly in eukaryotes. *Gene.* 313:17–42.

Geiger, C., W. Nagel, T. Boehm, Y. van Kooyk, C.G. Figdor, E. Kremmer, N. Hogg, L. Zeitlmann, H. Dierks, K.S. Weber, and W. Kolanus. 2000. Cytohesin-1 regulates beta-2 integrin-mediated adhesion through both ARF-GEF function and interaction with LFA-1. *EMBO J.* 19:2525–2536.

Guo, Q.M., R.L. Malek, S. Kim, C. Chiao, M. He, M. Ruffy, K. Sanka, N.H. Lee, C.V. Dang, and E.T. Liu. 2000. Identification of c-myc responsive genes using rat cDNA microarray. *Cancer Res.* 60:5922–5928.

Harnpicharnchai, P., J. Jakovljevic, E. Horsey, T. Miles, J. Roman, M. Rout, D. Meagher, B. Imai, Y. Guo, C.J. Brame, et al. 2001. Composition and functional characterization of yeast 66S ribosome assembly intermediates. *Mol. Cell.* 8:505–515.

Holland, E.C., N. Sonenberg, P.P. Pandolfi, and G. Thomas. 2004. Signaling control of mRNA translation in cancer pathogenesis. *Oncogene.* 23: 3138–3144.

Hölzel, M., F. Kohlhuber, I. Schlosser, D. Holzel, B. Luscher, and D. Eick. 2001. Myc/Max/Mad regulate the frequency but not the duration of productive cell cycles. *EMBO Rep.* 2:1125–1132.

Huh, W.K., J.V. Falvo, L.C. Gerke, A.S. Carroll, R.W. Howson, J.S. Weissman, and E.K. O'Shea. 2003. Global analysis of protein localization in budding yeast. *Nature.* 425:686–691.

Jin, A., K. Itahana, K. O'Keefe, and Y. Zhang. 2004. Inhibition of HDM2 and activation of p53 by ribosomal protein L23. *Mol. Cell. Biol.* 24:7669–7680.

Kim, S., Q. Li, C.V. Dang, and L.A. Lee. 2000. Induction of ribosomal genes and hepatocyte hypertrophy by adenovirus-mediated expression of c-Myc in vivo. *Proc. Natl. Acad. Sci. USA.* 97:11198–11202.

Lapik, Y.R., C.J. Fernandes, L.F. Lau, and D.G. Pestov. 2004. Physical and functional interaction between Pes1 and Bop1 in mammalian ribosome biogenesis. *Mol. Cell.* 15:17–29.

Li, Z., S. Van Calcar, C. Qu, W.K. Cavenee, M.Q. Zhang, and B. Ren. 2003. A global transcriptional regulatory role for c-Myc in Burkitt's lymphoma cells. *Proc. Natl. Acad. Sci. USA.* 100:8164–8169.

Lohrum, M.A., R.L. Ludwig, M.H. Kubbutat, M. Hanlon, and K.H. Vousden. 2003. Regulation of HDM2 activity by the ribosomal protein L11. *Cancer Cell.* 3:577–587.

Maiorana, A., X. Tu, G. Cheng, and R. Baserga. 2004. Role of pescadillo in the transformation and immortalization of mammalian cells. *Oncogene.* 23:7116–7124.

Marechal, V., B. Elenbaas, J. Piette, J.C. Nicolas, and A.J. Levine. 1994. The ribosomal L5 protein is associated with mdm-2 and mdm-2-p53 complexes. *Mol. Cell. Biol.* 14:7414–7420.

Nal, B., E. Mohr, M.I. Silva, R. Tagett, C. Navarro, P. Carroll, D. Depetris, C. Verthuy, B.R. Jordan, and P. Ferrier. 2002. Wdr12, a mouse gene encoding a novel WD-Repeat Protein with a notchless-like amino-terminal domain. *Genomics.* 79:77–86.

Nilsson, J.A., and J.L. Cleveland. 2003. Myc pathways provoking cell suicide and cancer. *Oncogene.* 22:9007–9021.

Oster, S.K., C.S. Ho, E.L. Soucie, and L.Z. Penn. 2002. The myc oncogene: MarvelouslY Complex. *Adv. Cancer Res.* 84:81–154.

Ouspenski, I.I., S.J. Elledge, and B.R. Brinkley. 1999. New yeast genes important for chromosome integrity and segregation identified by dosage effects on genome stability. *Nucleic Acids Res.* 27:3001–3008.

Patel, J.H., A.P. Loboda, M.K. Showe, L.C. Showe, and S.B. McMahon. 2004. Analysis of genomic targets reveals complex functions of MYC. *Nat. Rev. Cancer.* 4:562–568.

Pelengaris, S., and M. Khan. 2003. The many faces of c-MYC. *Arch. Biochem. Biophys.* 416:129–136.

Pestov, D.G., and L.F. Lau. 1994. Genetic selection of growth-inhibitory sequences in mammalian cells. *Proc. Natl. Acad. Sci. USA.* 91:12549–12553.

Pestov, D.G., Z. Strezoska, and L.F. Lau. 2001. Evidence of p53-dependent cross-talk between ribosome biogenesis and the cell cycle: effects of nucleolar protein Bop1 on G(1)/S transition. *Mol. Cell. Biol.* 21:4246–4255.

Polymenis, M., and E.V. Schmidt. 1999. Coordination of cell growth with cell division. *Curr. Opin. Genet. Dev.* 9:76–80.

Royet, J., T. Bouwmeester, and S.M. Cohen. 1998. Notchless encodes a novel WD40-repeat-containing protein that modulates Notch signaling activity. *EMBO J.* 17:7351–7360.

Rubbi, C.P., and J. Milner. 2003. Disruption of the nucleolus mediates stabilization of p53 in response to DNA damage and other stresses. *EMBO J.* 22:6068–6077.

Ruggero, D., and P.P. Pandolfi. 2003. Does the ribosome translate cancer? *Nat. Rev. Cancer.* 3:179–192.

Saveanu, C., A. Namane, P.E. Gleizes, A. Lebreton, J.C. Rousselle, J. Noaillac-Depeyre, N. Gas, A. Jacquier, and M. Fromont-Racine. 2003. Sequential protein association with nascent 60S ribosomal particles. *Mol. Cell. Biol.* 23:4449–4460.

Scheffner, M., J.M. Huibregtse, R.D. Vierstra, and P.M. Howley. 1993. The HPV-16 E6 and E6-AP complex functions as a ubiquitin-protein ligase in the ubiquitination of p53. *Cell.* 75:495–505.

Schlosser, I., M. Hölzel, M. Murnseer, H. Burtscher, U.H. Weidle, and D. Eick. 2003. A role for c-Myc in the regulation of ribosomal RNA processing. *Nucleic Acids Res.* 31:6148–6156.

Schmidt, E.V. 1999. The role of c-myc in cellular growth control. *Oncogene.* 18:2988–2996.

Schmidt, E.V. 2004. The role of c-myc in regulation of translation initiation. *Oncogene.* 23:3217–3221.

Schuhmacher, M., M.S. Staege, A. Pajic, A. Polack, U.H. Weidle, G.W. Bornkamm, D. Eick, and F. Kohlhuber. 1999. Control of cell growth by c-Myc in the absence of cell division. *Curr. Biol.* 9:1255–1258.

Schuhmacher, M., F. Kohlhuber, M. Hölzel, C. Kaiser, H. Burtscher, M. Jarsch, G.W. Bornkamm, G. Laux, A. Polack, U.H. Weidle, and D. Eick. 2001. The transcriptional program of a human B cell line in response to Myc. *Nucleic Acids Res.* 29:397–406.

Sherr, C.J., and J.D. Weber. 2000. The ARF/p53 pathway. *Curr. Opin. Genet. Dev.* 10:94–99.

Smith, T.F., C. Gaitatzes, K. Saxena, and E.J. Neer. 1999. The WD repeat: a common architecture for diverse functions. *Trends Biochem. Sci.* 24:181–185.

Stommel, J.M., N.D. Marchenko, G.S. Jimenez, U.M. Moll, T.J. Hope, and G.M. Wahl. 1999. A leucine-rich nuclear export signal in the p53 tetramerization domain: regulation of subcellular localization and p53 activity by NES masking. *EMBO J.* 18:1660–1672.

Strezoska, Z., D.G. Pestov, and L.F. Lau. 2002. Functional inactivation of the mouse nucleolar protein Bop1 inhibits multiple steps in pre-rRNA processing and blocks cell cycle progression. *J. Biol. Chem.* 277:29617–29625.

Sugimoto, M., M.L. Kuo, M.F. Roussel, and C.J. Sherr. 2003. Nucleolar Arf tumor suppressor inhibits ribosomal RNA processing. *Mol. Cell.* 11:415–424.

Takahashi, N., M. Yanagida, S. Fujiyama, T. Hayano, and T. Isobe. 2003. Proteomic snapshot analyses of preribosomal ribonucleoprotein complexes formed at various stages of ribosome biogenesis in yeast and mammalian cells. *Mass Spectrom. Rev.* 22:287–317.

Tao, W., and A.J. Levine. 1999a. Nucleocytoplasmic shuttling of oncoprotein Hdm2 is required for Hdm2-mediated degradation of p53. *Proc. Natl. Acad. Sci. USA.* 96:3077–3080.

Tao, W., and A.J. Levine. 1999b. P19(ARF) stabilizes p53 by blocking nucleocytoplasmic shuttling of Mdm2. *Proc. Natl. Acad. Sci. USA.* 96:6937–6941.

Thomas, G. 2000. An encore for ribosome biogenesis in the control of cell proliferation. *Nat. Cell Biol.* 2:E71–E72.

Trumpp, A., Y. Refaeli, T. Oskarsson, S. Gasser, M. Murphy, G.R. Martin, and J.M. Bishop. 2001. c-Myc regulates mammalian body size by controlling cell number but not cell size. *Nature.* 414:768–773.

Volarevic, S., M.J. Stewart, B. Ledermann, F. Zilberman, L. Terracciano, E. Montini, M. Grompe, S.C. Kozma, and G. Thomas. 2000. Proliferation, but not growth, blocked by conditional deletion of 40S ribosomal protein S6. *Science.* 288:2045–2047.

Wall, M.A., D.E. Coleman, E. Lee, J.A. Iniguez-Lluhi, B.A. Posner, A.G. Gilman, and S.R. Sprang. 1995. The structure of the G protein heterotrimer Gi alpha 1 beta 1 gamma 2. *Cell.* 83:1047–1058.

Weber, J.D., L.J. Taylor, M.F. Roussel, C.J. Sherr, and D. Bar-Sagi. 1999. Nucleolar Arf sequesters Mdm2 and activates p53. *Nat. Cell Biol.* 1:20–26.

Zhang, Y., G.W. Wolf, K. Bhat, A. Jin, T. Allio, W.A. Burkhart, and Y. Xiong. 2003. Ribosomal protein L11 negatively regulates oncoprotein MDM2 and mediates a p53-dependent ribosomal-stress checkpoint pathway. *Mol. Cell. Biol.* 23:8902–8912.